Clinical Journal of Gastroenterology (2019) 12:106–111
https://doi.org/10.1007/s12328-018-0917-6

CASE REPORT

# Caroli syndrome: a clinical case with detailed histopathological analysis

**Mikhail Mavlikeev[1] · Angelina Titova[1] · Renata Saitburkhanova[1] · Maria Abyzova[2] · Ilyas Sayfutdinov[3] · Nasima Gizzatullina[2,3] · Ilya Kotov[4] · Igor Plaksa[5,6] · Artur Isaev[6] · Sayar Abdulkhakov[1] · Andrey Kiyasov[1] · Roman Deev[6,7]**

Received: 15 September 2018 / Accepted: 15 October 2018 / Published online: 20 October 2018


**Abstract**
Herein we present a clinical case of the Caroli syndrome caused by the compound heterozygous mutation in the *PKHD1* gene. Histopathological assessment of liver detected biliary cirrhosis, numerous dilated bile ducts of various sizes, hyperplastic cholangiocytes containing a large amount of acid mucopolysaccharides, decreased ß-tubulin expression and increased proliferation of cholangiocytes. A significant proportion of hepatic tissue was composed of giant cysts lined with a single layer of cholangiocytes, containing pus and bile in its lumen and surrounded by granulation tissue. An accumulation of neutrophils in the lumen of the bile ducts was observed, as well as an infiltration of the ducts and cysts surrounding connective tissue by $CD4^+$ and to a lesser extent $CD8^+$ lymphocytes. This may be caused by the expression of HLA-DR by cholangiocytes. Atrophy and desquamation of the epithelium of collecting tubules with the formation of microcysts were detected in the kidneys without a clinically significant loss of renal function. Morphopathogenetic mechanisms of the Caroli syndrome can be targets for a potential pathogenetic therapy and prevention of its manifestations and complications.

**Keywords** Caroli syndrome · Fibrocystin · Ciliopathy · Histopathology

## Introduction

The Caroli syndrome (CS) is a rare (prevalence 1:1,000,000) autosomal recessive hereditary disease characterized by a cystic dilatation of the intrahepatic biliary ducts (IHBD) in combination with congenital portal fibrosis. The disease is caused by mutations in the *PKHD1* gene, which contains 67 exons and is localized in chromosome 6p21.1-p12. These mutations lead to a defect in the fibrocystin protein—a structural component of the primary cilia of the cholangiocytes—and cystogenesis [1].

There is a distinction between the CS and Caroli disease, which is characterized by isolated dilatation of large IHBD, the absence of congenital liver fibrosis, in which only one portion of the liver may be affected [2]. The syndrome and the disease were named after the French physician J.Caroli, who was the first to describe the manifestations of this condition without concomitant congenital fibrosis in detail (1958) [3].

## Case report

A male patient at the age of 37 was hospitalized with complaints of severe epigastric pain, nausea and vomiting. The patient suffered cirrhosis of the liver of unclear etiology since childhood (upon admission: Child–Pugh class B, Model for End-Stage Liver Disease (MELD) Score 43), and had manifestations of portal hypertension. The patient was infected by the human immunodeficiency virus (HIV), and his Hepatitis B, C was negative, while drug and alcohol use

✉ Mikhail Mavlikeev
mmavlikeev@gmail.com

1 Kazan (Volga region) Federal University, Kazan, Russia

2 Kazan State Medical University, Kazan, Russia

3 Interregional Clinical Diagnostic Center, Kazan, Russia

4 Genetics and Reproductive Medicine Center "GENETICO" Ltd, Moscow, Russia

5 Moscow City Oncological Hospital, No. 62, Moscow, Russia

6 Human Stem Cells Institute, Moscow, Russia

7 Ryazan State Medical University named after academician I.P. Pavlov, Ryazan, Russia

were denied. Upon ultrasound examination of the hepatobiliary system, slanting vertical dimension of the right lobe of the liver was 217 mm, left lobe − 123 mm, dimensions of the spleen were 315 × 123 mm, and enlargement of the gallbladder, as well as expansion of the common bile duct up to 19 mm were detected.

The results of clinical and biochemical blood analysis are presented in Table 1. The expansion of large IHBD was detected during the fistulography, and X-ray computer tomography (CT) detected numerous intrahepatic cysts and on the basis of the above, the clinical diagnosis of the CS was established (Fig. 1a).

After external trans-papillary drainage of the bile ducts (8 sessions on days 3, 4, 6, 9, 10, 11, 12, 13 of hospitalization), endoscopic sphincterotomy was performed with an extraction of small stones and putty bile. Antibiotic therapy (ceftriaxone, meropenem), detoxification, hepatoprotective, diuretic therapy, nutritional support and plasmapheresis were carried out.

There was an appearance of the ascitis from the 10th day of hospitalization and an abundant (2000–3500 ml/day) bile outflow through the nasopharyngeal drainage, as well as signs of dysmetabolic encephalopathy from the 24th day. On the 29th day of hospitalization, the patient fell into a coma and died.

On the day of death, the patient had leukocytosis, hyperbilirubinemia, an increase in the concentration of hepatic enzymes and creatinine (see Table 1).

A dense enlarged small-hummocky green–brown liver was observed during an autopsy. The cut section showed that the liver was knotty (nodes up to 0.3 cm), had enlarged IHBD and multiple multicameral cysts of 0.5–7.5 cm in diameter, filled with putty brown bile, white-yellowish pus and also has dense yellow-gray walls 0.1–0.5 cm in thickness (Fig. 1b). In addition, splenomegaly, cardiomegaly, an acute venous plethora of the lungs, widening of the lower third of the esophagus (up to 0.3 cm) were found. The kidneys were of normal size and did not contain cysts or other pathological changes (see Table 1). Death of patient was caused by dysmetabolic encephalopathy which led to brain edema confirmed by histological detection of pericellular and perivascular edema, cortical neurons degeneration.

Deoxyribonucleic acid (DNA) was isolated from paraffin-embedded liver tissue using the GeneJET formalin-fixed paraffin-embedded DNA Purification Kit (Thermo Fisher Scientific) according to manufacturer's instructions. The genomic DNA was enriched for target exome sequences using the paired-end amplification method (TruSeq Exome IDT, Illumina) and sequenced on the Illumina NovaSeq 6000 System. The resulting mean coverage of the target exome sequence was 237 ×, with 98.7% of exome having the coverage higher than 10×.

Sequencing data were analyzed using an automated algorithm that included the evaluation of the sequence quality (FASTQC module), removal of adapters and sequences with low quality (SEQPURGE module), reads alignment to the hg19 human genome (BWA MEM module), filtering of optical and polymerase chain reaction duplicates (SAMBLASTER module), optimization of the local alignment (module ABRA2), detection and quality filtering of variants (FREEBAYES package) and annotation of the variants with clinical information (ENSEMBL-VEP module). The

**Table 1** Indicators of blood tests and morphometry of the patient's organs

| Blood count | Day of admission | Day of death |
|---|---|---|
| Leucocytes, $\times 10^9$/l | 2.4 | 30.6 |
| Platelets, $\times 10^9$ l | 41.0 | 161.0 |
| Total bilirubin, μmol/l | 371.4 | 1108 |
| Direct bilirubin, μmol/l | 234.5 | 923.9 |
| Aspartate aminotransferase, U l | 50.0 | 127.0 |
| Alanine aminotransferase, U l | 26.0 | 82.0 |
| Gamma-glutamyltranspeptidase, U/l | 580.5 | 53.6 |
| Alkaline phosphatase | 730 | 433 |
| Creatinine, μmol/l | 100.98 | 153.61 |
| Morphometric index | | |
| Dimensions of the liver, cm | 30.0 × 19.0 × 23.0 × 12.0 | |
| Dimensions of the spleen, cm | 27.0 × 12.0 × 6.0 | |
| Spleen weight, g | 2100.0 | |
| Dimensions of the heart, cm | 18.0 × 11.0 × 5.0 | |
| The anterior wall of the left ventricle, cm | 3.0 | |
| Interventricular septum, cm | 2.5 | |
| The front wall of the right ventricle, cm | 0.7 | |
| Heart mass, g | 330.0 | |

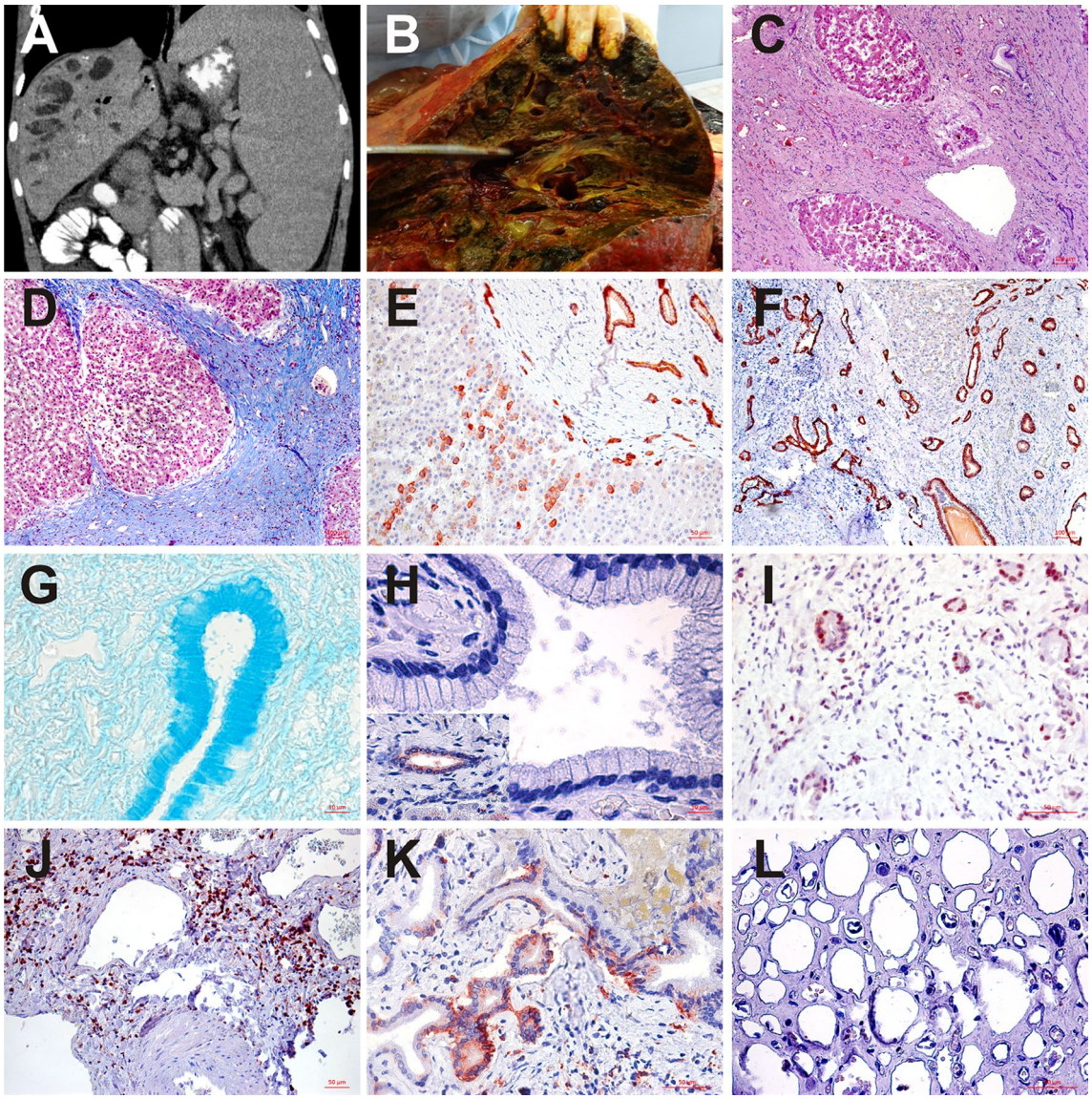


**Fig. 1** **a** X-ray CT in case of the CS, frontal section cut, arrow indicated giant liver cysts; **b** liver autopsy; **c** liver, hematoxylin and eosin staining; **d** liver, Mallory's trichrome staining; **e** liver, IHC reaction with antibodies to CK7; **f** liver, IHC reaction with antibodies to CK19; **g** liver, alcian blue staining, pH 2.5; **h** liver, IHC reaction with antibodies to ß-tubulin (insert-control); **i** liver, IHC reaction with antibodies to PCNA; **j** liver, IHC reaction with antibodies to CD4; **k** liver, IHC reaction with antibodies to HLA-DR; **l** kidney, hematoxylin and eosin staining

algorithm was tested on the Genome in a Bottle standard exome data, resulting in a sensitivity of 98.6% and the average specificity of 99.1%. The clinical relevance of the variants was interpreted according to the recommendations of American College of Medical Genetics and Genomics [4].

By sequencing the patient's exome, we observed three rare missense variants in the *PKHD1* gene leading to single amino acid substitutions in the fibrocystin: Tyr1136Cys, Arg1369Cys and Thr2869Lys (Table 2). The variant Tyr1136Cys was previously described as pathogenic [5] suggesting its role in the observed disease development. The substitution Thr2869Lys was repeatedly classified as (benign) polymorphism before [5] and therefore is very unlikely to be causal in our case. Given the very low population frequency and recessive inheritance of the syndrome, it is not surprising that the data for the Arg1369Cys pathogenicity is lacking. Taking into account that the clinical presentation is rather characteristic for the recessive CS, we conclude that this variant forms a compound heterozygote with the Tyr1136Cys variant.

Histopathological analysis of liver sections demonstrated biliary cirrhosis (Fig. 1c, d). There were signs of dysplasia of the hepatic tissue: hepatic parenchyma beam structure loss, hepatocyte heteromorphism, hyperchromism

**Table 2** The genetic variants discovered in the *PKHD1* gene

| Amino acid change | SNP ID number | Genomic change (hg19) cDNA change Protein change | Zygosity | Maximal population frequency (gnomAD) | Computer prediction | Evolutionary conservation | Classification of pathogenicity |
|---|---|---|---|---|---|---|---|
| Y1136C | rs41273726 | chr6:g.51893107T > C NM_138694:c.3407A > G NP_619639:p.Tyr1136Cys | Heterozygous | 1.853% | Moderately pathogenic | Non-conservative | Likely pathogenic |
| R1369C | rs368974211 | chr6:g.51890503G > A NM_138694:c.4105C > T NP_619639:p.Arg1369Cys | Heterozygous | 0.021% | MetaSVM: Benign FATHMM: Pathogenic | Non-conservative | Variant of uncertain significance |
| T2869K | rs142522748 | chr6:g.51637536G > T NM_138694:c.8606C > A NP_619639:p.Thr2869Lys | Heterozygous | 1.548% | Pathogenic | Conservative | Likely benign |

and polymorphism of their nuclei, as well as expression of cytokeratin (CK) 7 by hepatocytes (Fig. 1e). However, we did not find an expression of α-fetoprotein and bcl-2 by hepatocytes. At the same time, a diffuse expression of caspase-3 by hepatocytes was observed, that suggests a significant contribution of apoptosis to the development of pathological changes in the hepatic parenchyma.

Numerous bile ducts of various sizes were also detected in the fibrous fields (Fig. 1f), significantly expanded (cross-sectional area 243.66 (154.36, 466.54) μm$^2$, 40.30 (28.20, 58.85) μm$^2$ in control, $p < 0.05$), with wall ruptures, containing gallstones and pus. Hyperplasic cholangiocytes contained a large number of acid mucopolysaccharides (Fig. 1g). Staining with antibodies to β-tubulin showed a decrease in its expression in the liver cholangiocytes compared to the control (Fig. 1h).

Proliferation of cholangiocytes was detected with anti-proliferating cells nuclear antigen (PCNA) staining, and the number of bile ducts in the patient's liver [10 (7; 13.5)] did not differ significantly from the control [14.5 (11.5, 16.5) ($p > 0.05$)], which is associated with the presence of periportal fibrosis and with the impairment of liver histoarchitecture (Fig. 1i).

A significant proportion of hepatic tissue was composed of giant cysts lined with a single layer of cholangiocytes, containing pus and bile in its lumen and surrounded by granulation tissue. There was an accumulation of neutrophils in the lumen of the bile ducts, also an infiltration of the ducts and the walls of cysts surrounding connective tissue CD4$^+$ and to a lesser extent CD8$^+$ lymphocytes (Fig. 1j). This may be caused by the expression of human leukocyte antigen DR isotype (HLA-DR) by cholangiocytes, detected immunohistochemically, and this was not observed in control (Fig. 1k). Immunohistochemical (IHC) reaction with antibodies to CD68 revealed Kupffer cells increased in number and size, phagocytising bile.

Atrophy and desquamation of the epithelium of collecting tubules with the formation of microcysts were detected in the kidneys, as well as a venous plethora of the renal medulla (Fig. 1l).

## Discussion

The development of IHBD occurs from the layer of CK7$^+$/CK19$^+$ cells of the future hepatic parenchyma—ductal plate [1]. There are few primary cilia on the apical membrane of the cholangiocytes (as well as the tubular epithelium of the kidney) that react to the fluid flow and contain the mechanosensitive calcium channels formed by a complex of polycystin-2 and fibrocystin proteins [6]. Mutations in the *PKHD1* gene, accompanied by a loss of fibrocystin, lead to a shortening and deformation of the primary cilia, a disruption of the calcium channels, a decrease in the intracellular calcium level, a switch from the noncanonical to the canonical Wnt signaling pathway, a distortion of the planar cell polarity and remodeling of the ductal plate, persistence of its residues—the so-called malformation of the ductal plate [1].

Disruption of the structure and function of primary cilia also takes effect after birth as a disruption of differentiation and excessive proliferation of cholangiocytes. Terminal differentiation of cholangiocytes is normally stimulated by the expression of the transcription factors Foxa1 and Foxa2 that suppress the autocrine secretion of promitotic interleukin (IL) 6 by cholangiocytes [7]. The absence of cholangiocytes maturation in case of the CS can cause increased proliferation of cholangiocytes, as well as peribiliary fibrosis and inflammation due to the paracrine effect of IL-6 on leukocytes and myofibroblasts [8]. The combination of a low differentiation and a pro-inflammatory and profibrogenic phenotype of cholangiocytes is also observed in adults with bile duct damage [9].

The persistence of low differentiated cholangiocytes causes their sensitivity to the ligands of the Hedgehog (Hh) signaling pathway and can cause congenital fibrosis due to the secretion of pro-inflammatory and profibrogenic chemokine monocyte chemoattractant protein 1 (MCP-1) and IL-13 [10].

The reason for the rich vascularization of the cyst walls in case of the CS is the increased expression of proangiogenic factors by cholangiocytes, for instance, vascular endothelial growth factor A (VEGF-A) due to the hyperactivation of the MEK/ERK/2/mTOR signaling pathway [11].

Major histocompatibility complex (MHC) class II molecules, usually expressed in antigen-presenting cells, are also observed on epithelium in cases of some autoimmune diseases, for instance, primary biliary cirrhosis [12] and may be the cause of the formation of secondary biliary cirrhosis in the case of the patient with the CS.

Histopathological analysis of the liver of the patient with the CS detected hyperplastic cholangiocytes overcrowded with acidic mucopolysaccharides. In addition to the mechanosensory, the role of primary cilia in cholangiocytes is also chemo- and osmodetection of the bile composition [13]. Our data suggest that the loss of fibrocystin leads to the increase of cholangiocytes volume, presumably because of the secretion disruption of ions and water. Whether this causes a secondary disturbance of osmolarity and the pH of the bile and whether it contributes to cystogenesis, the formation of gallstones and the development of chronic cholangitis in cases of the CS, requires further study.

The CS patients have more than a hundredfold increase of the risk of developing cholangiocarcinoma associated not only with chronic inflammation [14], but also a low level of differentiation and increased proliferative activity of cholangiocytes, hyperactivation of the Hh signaling pathway, which is also common for cholangiocarcinoma, cell polarity and the mitotic spindle correct orientation disorder due to the abnormal structure of the primary cilia, which leads to the formation of polyploidy and chromosomal instability [15]. It was constituted that somatic mutations of the *PKHD1* gene occur in colon carcinoma cells with high frequency [16], abd there is a mention of the combination of familial adenomatous polyposis and the CS [17], as well as a significant correlation between polycystic kidney and malignant tumors of the liver, kidneys and colon [18], which indicates that patients with the CS have the predisposition to the development of other malignant neoplasms aside from cholangiocarcinoma.

The *PKHD1* spans over 469 kb and is one of the largest in the human genome. More than 700 different mutations in *PKHD1* have been described, among them more than 200 pathogenic or likely pathogenic (Online Mendelian Inheritance in Man (OMIM) 606,702). The mutations found in the patient lead to amino acid substitutions (p.Tyr1136Cys and p.Arg1369Cys), in both cases this leads to the replacement of the polar amino acid by the less polar in the extracellular domains IPT/TIG 6 (atypical) and IPT/TIG 8 (atypical), while the second variant is located in the area predicted as an exonic splicing enhancer, changes in which can affect the splicing process and, consequently, change the normal process of protein synthesis. The reasons why some mutations of the *PKHD1* gene manifest themselves with a combination of polycystic kidney disease and congenital fibrosis of the liver or the CS, have not yet been established; however, this gene has a very complex splicing pattern and various mutations can disrupt the organ-specific balance of expression of different isoforms. It is important to note that in the case presented by us the patient had no functional changes of the kidneys, however, histopathological analysis revealed the kidneys' involvement in form of microcyst formation in the medulla.

Thus, dysplasia and excessive proliferation of cholangiocytes due to disruption of the structure and function of primary cilia are important pathomorphogenetic components of the CS. The rich vascularization of cysts, severe portal fibrosis with marked lymphocytic infiltration is caused by the proangiogenic, profibrogenic and pro-inflammatory phenotypes of low differentiated cholangiocytes. The mechanisms and signaling pathways involved in cysto- and carcinogenesis can be targeted for potential pathogenetic therapy and prevention of manifestations and complications of the CS.

**Author contributions** Authors MOM, APK and RVD conceived and designed the study, and wrote, edited and reviewed the manuscript. Authors AAT, RRS, MSA, ILP performed histological analysis, and reviewed the manuscript. Authors IMS, NFG, SRA performed clinical examination and reviewed the manuscript. Authors INK, AAI performed genetic analysis and reviewed the manuscript. All authors gave final approval for publication. Author MMO takes full responsibility for the work as a whole, including the study design, access to data and the decision to submit and publish the manuscript.

**Funding** The work is performed according to the Russian Government Program of Competitive Growth of Kazan Federal University.

## Compliance with ethical standards

**Conflict of interest** The authors declare that they have no conflict of interest.

**Human rights** All procedures followed have been performed in accordance with the ethical standards laid down in the 1964 Declaration of Helsinki and its later amendments.

**Informed consent** Consent cannot be obtained because the patient is dead, and the parents/guardian cannot be traced. This study does not contain identifying information of the patients.

## References


1. Strazzabosco M, Fabris L. Development of the bile ducts: essentials for the clinical hepatologist. J Hepatol. 2012;56:1159–70.
2. Kerkar N, Norton K, Suchy FJ. The hepatic fibrocystic diseases. Clin Liver Dis. 2006;10:55–71.
3. Caroli J, Soupalt R, Kossakowski J, et al. La dilatation polykystique congenitale des voies biliaires intrahepatiques. Essai del classification Sem Hop Paris. 1958;34:488–95.
4. Richards S, Aziz N, Bale S, et al. Standards and guidelines for the interpretation of sequence variants: a joint consensus recommendation of the american college of medical genetics and genomics and the association for molecular pathology. Genet Med. 2015;17:405–24.
5. Sharp AM, Messiaen LM, Page G, et al. Comprehensive genomic analysis of PKHD1 mutations in ARPKD cohorts. J Med Genet. 2005;42:336–49.
6. Ward CJ, Yuan D, Masyuk TV, et al. Cellular and subcellular localization of the ARPKD protein; fibrocystin is expressed on primary cilia. Hum Mol Genet. 2003;12:2703–10.
7. Li Z, White P, Tuteja G, et al. Foxa1 and Foxa2 regulate bile duct development in mice. J Clin Invest. 2009;119:1537–45.
8. Fabris L, Strazzabosco M. Epithelial-mesenchymal interactions in biliary diseases. Semin Liver Dis. 2011;31:11–32.
9. Roskams T, Theise ND, Balabaud C, et al. Nomenclature of the finer branches of the biliary tree: canals, ductules, and ductular reactions in human livers. Hepatology. 2004;39:1739–45.
10. Omenetti A, Syn WK, Jung Y, et al. Repair-related activation of hedgehog signaling promotes cholangiocyte chemokine production. Hepatology. 2009;50:518–27.
11. Spirli C, Okolicsanyi S, Fiorotto R, et al. ERK1/2-dependent vascular endothelial growth factor signaling sustains cyst growth in polycystin-2 defective mice. Gastroenterology. 2010;138:360–71.
12. Nishimoto H, Yamada G, Mizuno M, et al. Immunoelectron microscopic localization of MHC class 1 and 2 antigens on bile duct epithelial cells in patients with primary biliary cirrhosis. Acta Med Okayama. 1994;48:317–22.
13. Masyuk AI, Gradilone SA, Banales JM, et al. Cholangiocyte primary cilia are chemosensory organelles that detect biliary nucleotides via P2Y12 purinergic receptors. Am J Physiol Gastrointest Liver Physiol. 2008;295:G725-34.
14. Jang MH, Lee YJ, Kim H. Intrahepatic cholangiocarcinoma arising in Caroli's disease. Clin Mol Hepatol. 2014;20:402–5.
15. AbouAlaiwi WA, Ratnam S, Booth RL, et al. Endothelial cells from humans and mice with polycystic kidney disease are characterized by polyploidy and chromosome segregation defects through survivin down-regulation. Hum Mol Genet. 2011;20:354–67.
16. Sjoblom T, Jones S, Wood LD, et al. The consensus coding sequences of human breast and colorectal cancers. Science. 2006;314:268–74.
17. Hodgson SV, Coonar AS, Hanson PJ, et al. Two cases of 5q deletions in patients with familial adenomatous polyposis: possible link with Caroli's disease. J Med Genet. 1993;30:369–75.
18. Yu TM, Chuang YW, Yu MC, et al. Risk of cancer in patients with polycystic kidney disease: a propensity-score matched analysis of a nationwide, population-based cohort study. Lancet Oncol. 2016;17:1419–25.